Hindawi
Geofluids
Volume 2023, Article ID 9786775, 10 pages
https://doi.org/10.1155/2023/9786775

Research Article

Theoretical and Experimental Antiscaling Performance Study of Several Inhibitors to Prevent Barium Sulfate Formation during Water Injection in Oil Reservoirs

Haitao Li and Ran Li

Key Laboratory of Reservoir Geology and Development Engineering, Southwest Petroleum University, Chengdu 610500, China

Correspondence should be addressed to Ran Li; 316920020@qq.com

Received 28 July 2022; Revised 19 October 2022; Accepted 24 November 2022; Published 20 January 2023

Academic Editor: Yuxiang Zhang

Copyright © 2023 Haitao Li and Ran Li. This is an open access article distributed under the Creative Commons Attribution License, which permits unrestricted use, distribution, and reproduction in any medium, provided the original work is properly cited.

One of the hazards from mineral precipitation during oilfield production is scaling, which mainly manifests in the following three aspects: it leads to reduction in permeability, in deliverability, and in water intake capacity of reservoir; the flowing area of pipeline shrinks, which could elevate the fluid flow resistance and even lead to well shut; and scaling could also contribute to pressure loss and may cause tube blasting when it is serious. Therefore, scaling not only improves production costs but also poses a serious threat to production safety. The injection of scale inhibitors in the process of water flooding is the main method to combat scale build-up. Efficiency of inhibitor or adsorption between inhibitor and scale is the key factor that determines success or failure of the scale inhibitor squeeze treatments. Previous studies have confirmed that interaction between the inhibitor and the scale surface plays an important role in scale prevention and control. Although many studies have been carried out on inhibitor efficiency and inhibition mechanism, a comprehensive understanding of inhibitor-scale interaction is yet available and the adsorption behavior between inhibitor and scale surface requires further research. Thereupon, this study presents performance evaluation and computational study of three inhibitors, including EDTMPS, DTPMP, and DTPA-5Na based on the scaling prediction result of the Huaqing oilfield. It was found that $BaSO_4$ was the main type of scaling and the antiscaling performance of the three inhibitors was experimentally displayed as DTPA-5Na > DTMP > EDTMPS at the concentration from 40 mg/L to 120 mg/L. SEM micrographs of $BaSO_4$ surfaces in the absence and presence of inhibitors at the concentration of 80 mg/L showed that the inhibitors obviously influenced the process of crystal growth of $BaSO_4$ by lattice distortion and chelate effect. In addition, density functional theory (DFT) calculations unraveled that adsorption capacity of inhibitors interacting with three surfaces of $BaSO_4$ increased in the order of DTPA-5Na > EDTMPS > DTPMP. DPTA-5Na was likely to be chemisorbed on the surfaces of $BaSO_4$ while DTPMP and EDTMPS tended to be adsorbed on (210) and (001) surfaces of $BaSO_4$ by chemical and physical effect, respectively. Calculation of difference charges and DOS analysis indicated that DTPA-5Na interacted with $BaSO_4$ by combining atoms of oxygen and sodium to form new chemical bonds while EDTMPS and DTPMP interacted with $BaSO_4$ by combining hydrogen and oxygen atoms to form physical bonds. The research results can provide a better understanding of the interaction between inhibitors and scale surfaces and can also lay scientific foundation for barite scale prevention and further development of inhibitors.

1. Introduction

Waterflooding in oil industry is essential to oil production, for it supplies producing energy and thus improves the efficiency of development. However, it also brings problems, such as scaling and corrosion, which may pose a big threat to the oilfield system [1].In the injection process, inorganic and organic solids could form in the reservoir, wellbore, surface pipelines, and pump [2, 3], thus damaging the formation and reducing production. Moreover, equipment is likely to be impaired, which results in a significant rise in production costs [4, 5].The precipitation of carbonate and sulfate scale is the main inorganic scales existing in oil reservoirs and producing wells [6, 7]. At present, a set of effective

Table 1: Ionic composition of formation water and injection water.

Brines	pH	Ion content (mg/L)								Salinity (mg/L)
		Ca^{2+}	Mg^{2+}	Ba^{2+}	Na^{+}	K^{+}	Cl^{-}	HCO_3^{-}	SO_4^{2-}	
Q2	7.7	69	94	0	1128	5	703	93	2736	5035
L49-07	7.5	268	814	1221	35015	420	65233	192	0	109415

Table 2: Ionic composition of synthetic formation and injection water.

Brines	pH	Ion content (mg/L)						Salinity (mg/L)
		Ba^{2+}	Na^{+}	K^{+}	Cl^{-}	HCO_3^{-}	SO_4^{2-}	
Q2	7.7	0	1128	5	703	93	2736	5035
L49-07	7.5	1221	35015	420	65233	192	0	109415

prevention plans has been established to prevent and remove calcium carbonate and calcium sulfate. Nevertheless, it is still difficult to deal with barium sulfate scale because it is insoluble in most fluids and cannot be dissolved by any acid [8].

Inhibitor-squeezing treatment is the most economical and efficient approach to prevent scale deposition in oilfields. A variety of scale inhibitors has been developed up to now. Scale inhibitors, which contain phosphonates and organophosphorus compounds, are widely used because of their good antiscaling performance [9].With the reinforcement of environmental protection policies, development of eco-friendly scale inhibitors becomes inevitable [10–12]. Efficiency of scaling inhibitors can be affected by the concentration of brines ions, solution pH, temperature, and pressure. The static antiscaling experiment is often used in the laboratory to evaluate performance of scale inhibitors [13–15]. But, it is difficult to analyze the mechanism of interaction between inhibitors and scales by static jar tests. Therefore, it is urgent to develop new methods to analyze inhibition mechanism so as to assess the performance of inhibitors. In recent years, molecular simulation is used to predict the antiscaling efficiency of new inhibitors and study their adsorption mechanism on scale surfaces [16, 17]. However, development of efficient inhibitors and mechanism research still presents a serious challenge, especially when the conditions of oilfields get increasingly complicated and environmental constraints require that inhibitors are heat-resistant and capable of biodegradation with a low toxicity.

In this research, the antiscaling performance of several inhibitors, including diethylene triamine penta (DTPMP), ethylene diamine tetra sodium (EDTMPS), and sodium diethylene triamine pentacetate (DTPA-5Na), was evaluated by static antiscaling experiments based on the prediction of scaling tendency of the Huaqing oilfield. Then, the morphology of scale surfaces in the presence and absence of inhibitors was observed by scanning electron microscope. In addition, the adsorption strength and sites of inhibitors interacting with the three surfaces of barium sulfate were studied by the density functional theory method. The obtained results could benefit the inhibition performance for $BaSO_4$ scale control in oilfield operations.

2. Experimental and Computational Details

2.1. Scaling Prediction. Scaling prediction work aimed at forecasting the dominant type of scales and the scaling tendency of the oilfield. The prediction work was finished by a commercial software package (OLI ScaleChem), based on the analysis result of ion composition of the injection water (Q2) and formation water (L49-07) of the Huaqing oilfield (Table 1). Factors, including temperature (75°C) and pressure (8 MPa), were taken into account. The mixing ratio of injection water and formation water ranged from 1 : 9 to 9 : 1.

2.2. Antiscaling Evaluation Experiments

2.2.1. Experimental Materials. The materials used in this experiment are calcium chloride, magnesium chloride hexahydrate, potassium chloride, barium chloride dihydrate, sodium sulfate, sodium bicarbonate, sodium carbonate, sodium chloride, ammonium chloride, ethylene diamine tetraacetic acid (EDTA), and eriochrome black T, all of which were obtained from Kelong Chemical Co. (Chengdu, China) and AR analytical reagent grade. Inhibitors, including diethylene triamine penta (DTPMP), ethylene diamine tetra sodium (EDTMPS), and sodium diethylene triamine pentaacetate (DTPA-5Na), were purchased from Oriental Chemical Co. (Zouping, China).

2.2.2. Preparation of Synthetic Injection Water and Formation Water. Synthetic injection water and formation water were prepared according to the result of scaling prediction work. In order to obviate the interferences of other types of scale which might affect the accuracy of result, brine compositions were partially adjusted, which is shown in Table 2. NaCl, KCl, Na_2SO_4, $NaHCO_3$, $BaCl_2$, H_2O, and Na_2CO_3 were used to prepare the synthetic injection and formation water. The predetermined amounts of the salts were dissolved in deionized water to produce the synthetic brines. In order to ensure the brines were stable, they were set still for 24 hours after being stirred by a magnetic stirrer.

2.2.3. Injection Water Being Mixed with Formation Water. Firstly, synthetic injection water was mixed with formation water which contained only anions in the absence and presence of DTPA-5Na, EDTMPS, and DTPMP in pressure

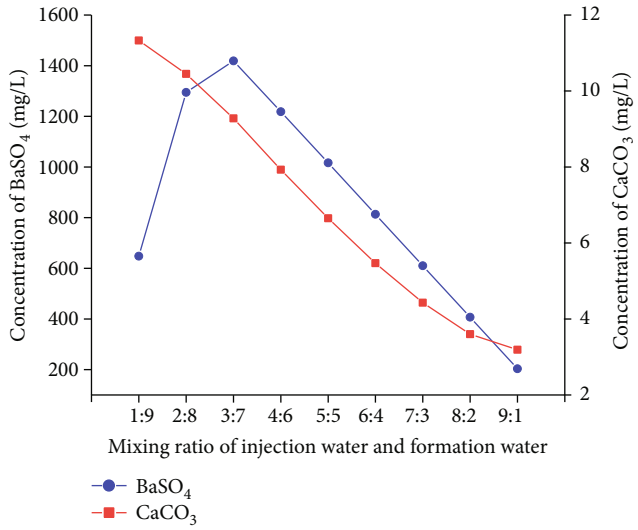

Figure 1: Scaling type and tendency of mixed water at different mixing ratio (Q2:L49-07).

tanks, respectively. Secondly, the tanks were preheated in the water bath at 75°C for 30 min. Thirdly, the tanks were opened and filled with synthetic injection and formation water which contained only cations. Lastly, the tanks were sealed, and a high-pressure nitrogen gas bottle was used to pressurize them to 8 MPa. The tanks were submerged in the water bath at 75°C for 26 h.

2.2.4. Inhibition Efficiency Calculation. The tanks were taken out from the thermostatic bath and the inverse titration method was applied to calculate the concentration of Ba^{2+}; then, the efficiency of inhibitors was evaluated. This experiment mainly referred to the Chinese petroleum and natural gas industry standard SY/5673-2020 "General technical conditions of scale inhibitors for oil fields" to evaluate the antiscaling performance of the inhibitors.

The antiscaling efficiency of the inhibitors is derived from the following equation [18]:

$$E = \frac{c_2 - c_1}{\gamma c_0 - c_1} \times 100\%, \tag{1}$$

where c_0 stands for the concentration of barium ions before injection water was mixed with the formation water in mol/L. c_1 represents the concentration of barium ions in the absence of inhibitors in mol/L. c_2 is the concentration of barium ions in the presence of inhibitors in mol/L. γ is the volume fraction of barium ions when two fluids were mixed.

The concentration of barium ions is derived from

$$C_{Ba^{2+}} = \frac{V_{EDTA} \cdot C_{ETDA} - V_{Mg^{2+}} \cdot C_{Mg^{2+}}}{V}, \tag{2}$$

where V represents the volume of measured sample in mL. V_{EDTA} and $V_{Mg^{2+}}$ are the dosage of EDTA and magnesium standard solution in mL, respectively.

The volume fraction of barium ions is defined as follows:

$$\gamma = \frac{V_{Ba^{2+}}}{V_{sum}} = \frac{V_{Ba^{2+}}}{V_{Ba^{2+}} + V_{SO_4^{2-}}}. \tag{3}$$

2.3. Surface Characterization. The surface morphology of barium sulfate before and after interacting with 80 mg/L of inhibitors, including DTPA-5Na, EDTMPS, and DTPMP was observed by the scanning electron microscopy (Quanta 450, Thermo, the United States). SEM micrographs had been recorded at a magnification of 2000 × and at an accelerating voltage of 20 kV. All samples were cleaned and dried for 24 h; then, they were used to conduct the SEM examination.

2.4. Molecular Simulation. The molecular modeling method was applied to select the most effective inhibitor which also had a good antiscaling performance in the evaluation experiment. The theoretical study of the antiscaling ability of DTPA-5Na, EDTMPS, and DTPMP for $BaSO_4$ was conducted with molecular simulation. All molecular systems were geometrically optimized by Density Functional Theory (DFT) using the Materials Studio software interface through $DMol^3$ suites [19, 20]. Molecular geometries of DPTA-5Na, EDTMPS, and DTPMP models, as well as of the systems which consisted of inhibitors and barium sulfate surfaces, were optimized through DFT energy minimizations using the GGA/PBE functional [21] with the DND basis set, and all calculations were accomplished under spin unrestricted conditions. In order to accelerate convergence while retaining accuracy, the value of smearing was set at 0.005 Ha. All geometries kept being optimized until convergence tolerance, maximum force, and maximum displacement were less than 1×10^{-4} Ha, 0.02 Ha/Å, and 0.05 Å, respectively.

The adsorption energy E_{ads} is defined as the total energy of the adsorption system minus the energy of the inhibitors and scale surface. The formula is shown as

$$E_{ads} = E_{total} - E_{surface} - E_{inhibitor}, \tag{4}$$

where E_{total}, $E_{surface}$, and $E_{inhibitor}$ are total energy of the adsorption system, energy of inhibitors, and energy of scale surface, respectively.

According to the model proposed by Allan et al. [22], the (210), (001), and (101) surfaces as the three most stable surfaces of $BaSO_4$ were selected to simulate the adsorption process in this study. DTPA-5Na, EDTMPS, and DTPMP were placed separately on the three exposed surfaces of the $BaSO_4$ slabs contained in the following periodic simulations cells: the $BaSO_4$ (210) surface (cell parameters $a = 14.290$, $b = 28.106$, and $c = 17.519$ Å); the $BaSO_4$ (001) surface (cell parameters $a = 17.740$, $b = 10.900$, and $c = 18.435$ Å); and the $BaSO_4$ (101) surface (cell parameters $a = 22.780$, $b = 10.900$, and $c = 17.252$ Å). These dimensions were sufficient to fully allocate all atoms adsorbed on scale surfaces.

After that, the (001) surface of barium sulfate was chosen to locate adsorption sites according to the calculation results of adsorption energy of the system consisting of inhibitors and scale surfaces. This procedure was finished by analysis

Table 3: Efficiency of inhibitors at different concentrations.

Inhibitors	Mixing ratio	Temperature (°C)	Pressure (MPa)	Concentration (mg/L)	Efficiency (%)
DTPMP	3 : 7	75	8	40	40.96
DTPMP	3 : 7	75	8	50	45.61
DTPMP	3 : 7	75	8	60	51.88
DTPMP	3 : 7	75	8	70	57.32
DTPMP	3 : 7	75	8	80	62.63
DTPMP	3 : 7	75	8	90	67.91
DTPMP	3 : 7	75	8	100	70.35
DTPMP	3 : 7	75	8	110	71.73
DTPMP	3 : 7	75	8	120	72.01
EDTMPS	3 : 7	75	8	40	30.78
EDTMPS	3 : 7	75	8	50	37.13
EDTMPS	3 : 7	75	8	60	47.76
EDTMPS	3 : 7	75	8	70	56.67
EDTMPS	3 : 7	75	8	80	60.05
EDTMPS	3 : 7	75	8	90	66.44
EDTMPS	3 : 7	75	8	100	68.96
EDTMPS	3 : 7	75	8	110	70.85
EDTMPS	3 : 7	75	8	120	71.01
DTPA5Na	3 : 7	75	8	40	46.49
DTPA5Na	3 : 7	75	8	50	51.33
DTPA5Na	3 : 7	75	8	60	57.90
DTPA5Na	3 : 7	75	8	70	60.11
DTPA5Na	3 : 7	75	8	80	65.35
DTPA5Na	3 : 7	75	8	90	68.37
DTPA5Na	3 : 7	75	8	100	73.36
DTPA5Na	3 : 7	75	8	110	77.99
DTPA5Na	3 : 7	75	8	120	78.13

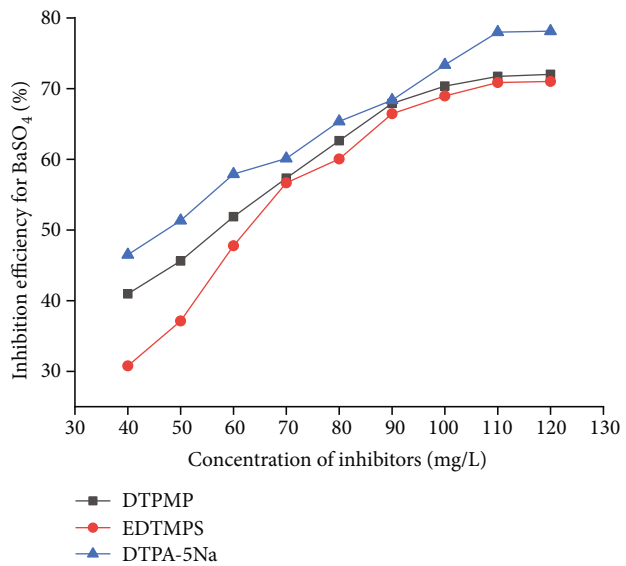

Figure 2: The antiscaling performance of several inhibitors for $BaSO_4$ at different concentrations.

of difference charge. Lastly, DOS analysis provided evidence of adsorption sites, which could explain the new bonds combining the inhibitors with barium sulfate.

3. Results and Discussion

3.1. Scaling Prediction. The scaling prediction was made based on the analysis result of ionic composition of Q2 and L49-07 (Table 1). Figure 1 shows the type and tendency of the scaling when injection water was mixed with formation water in different proportions under a constant pressure of 8 MPa and temperature of 75°C, respectively. It can be found that barium sulfate is the main composition of scales. The quantity of $BaSO_4$ increases with the rise of the mixing ratio of the two fluids within the range from 1 : 9 to 3 : 7. The quantity of $BaSO_4$ reaches maximum when the ratio of injection water and formation water is 3 : 7.Then it decreases with the fall of the ratios of injection water to formation water. This can be ascribed to the sufficient reaction between barium ions and sulfate ions when injection water and formation water are mixed with a ratio of 3 : 7. Then the decreasing quantity of $BaSO_4$ can be explained by the decline of Ba^{2+} levels which are supplied by formation water [23].

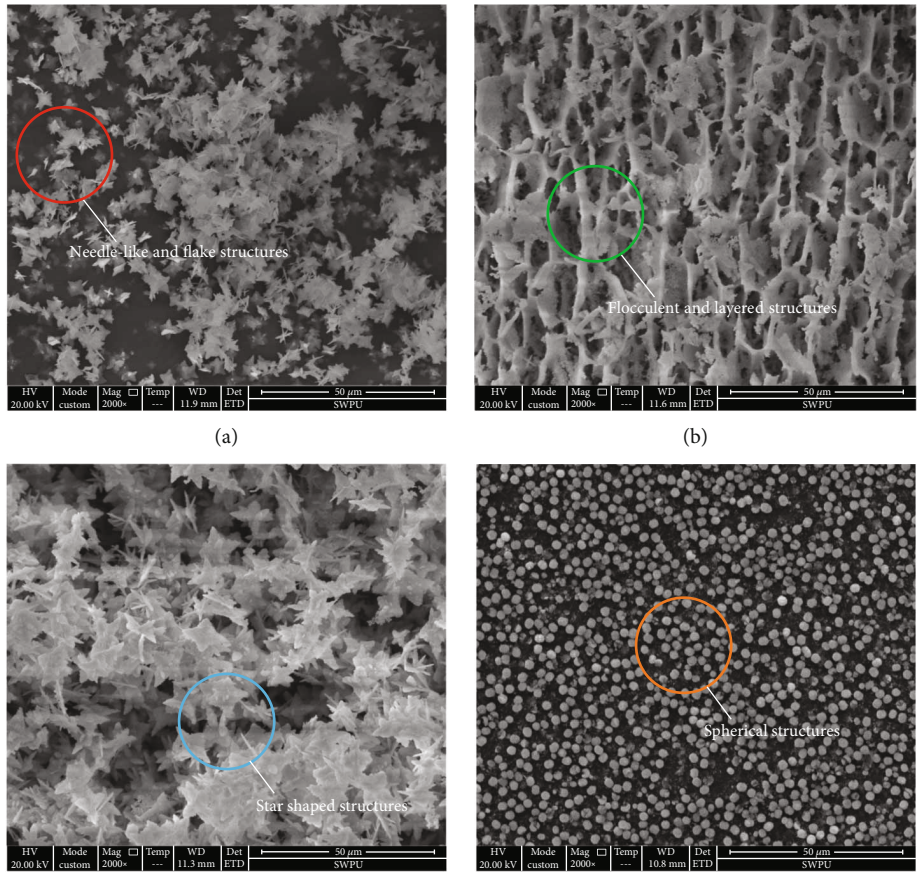

Figure 3: SEM micrographs of $BaSO_4$ precipitates (a) in the absence of inhibitor, (b) in the presence of 80 mg/L of DTPMP, (c) in the presence of 80 mg/L EDTMPS, and (d) in the presence of 80 mg/L DTPA-5Na.

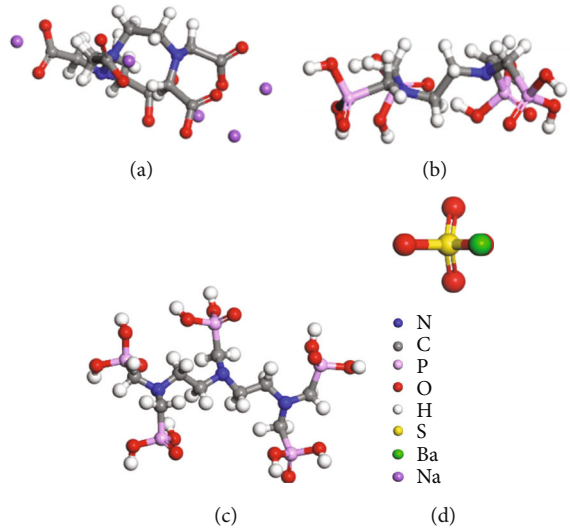

Figure 4: Molecular models of inhibitors and mineral scale (a) DTPA-5Na, (b) EDTMPS, (c) DTPMP, and (d) $BaSO_4$.

3.2. Antiscaling Experiment. The antiscaling experiment results show different performances of these inhibitors at several concentrations under static conditions (Table 3 and Figure 2). The efficiency of DTPMP, EDTMPS, and DTPA-5Na increases dramatically with concentrations increasing within the range between 40 mg/L and 110 mg/L, then rises slightly from 71.73% to 72.01%, 70.85% to 71.01%, and 77.99% to 78.13%, respectively. Crystal growth

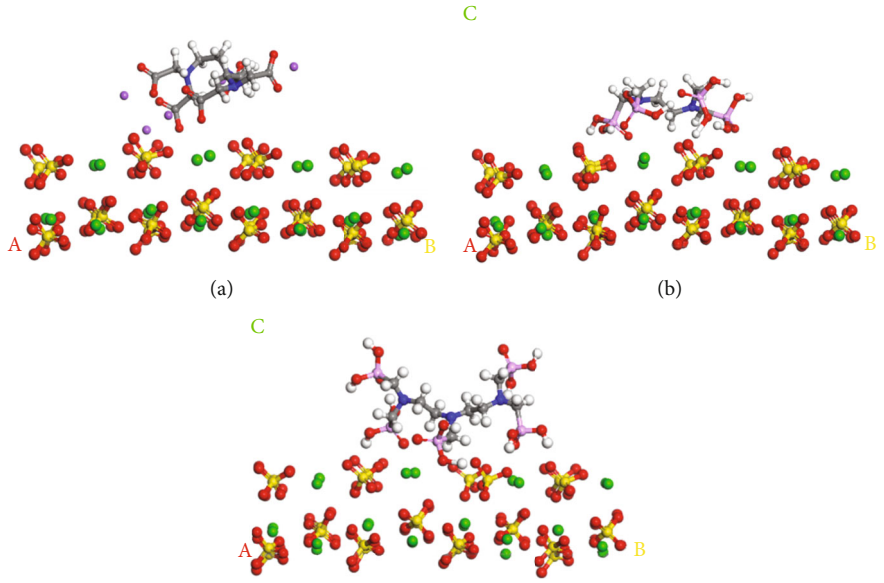

Figure 5: (210) Surface of barium sulfate is interacting with (a_1) DPTA-5Na, (b_1) EDTMPS, and (c_1) DTPMP.

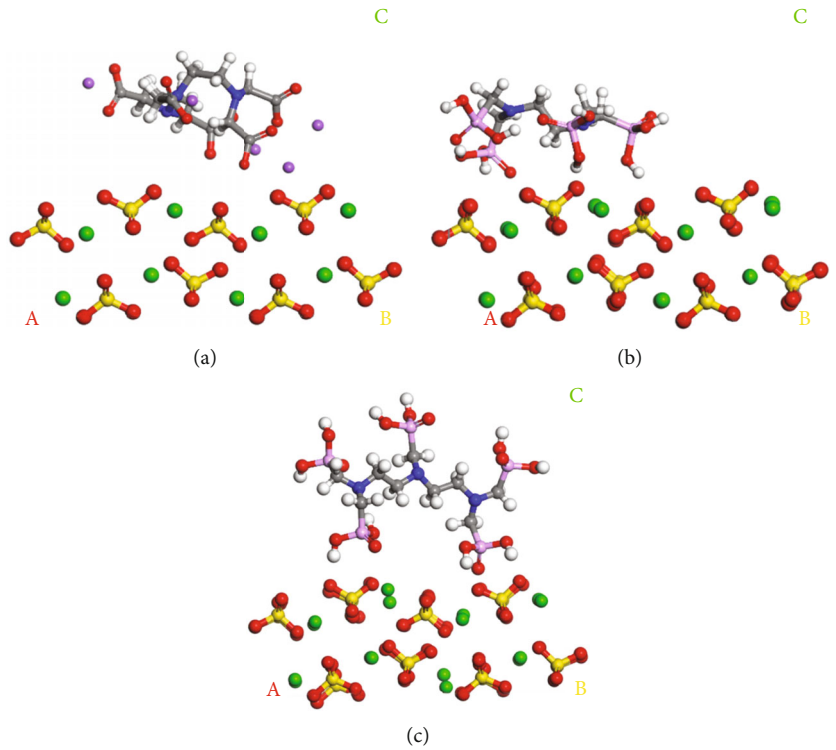

Figure 6: (001) Surface of barium sulfate is interacting with (a_2) DPTA-5Na, (b_2) EDTMPS, and (c_2) DTPMP.

is inhibited when the active points are covered by molecules of inhibitor absorbed on them, which makes the nearby lattice "misplaced" [24]. Hence, efficiency increases significantly with concentrations increasing because more active growth points are covered when the concentrations of the inhibitors are less than 110 mg/L. According to the theory about screw dislocations of crystal [25], the number of active growth points on crystal surface is restricted. Therefore, the efficiency rises slightly when the concentration of the inhibitors is above 110 mg/L. The efficiency is low while the concentrations of DTPMP and EDTMPS are less than 50 mg/L. By contrast, DTPA-5Na has better performance than DTPMP and EDTMPS at the same concentration. Moreover, DTPA-5Na is also demonstrated to be the most efficient in fighting scaling when concentration is above 60 mg/L.

3.3. Surface Characterization. Figure 3 shows the morphology changes during the growth of $BaSO_4$ crystal precipitates

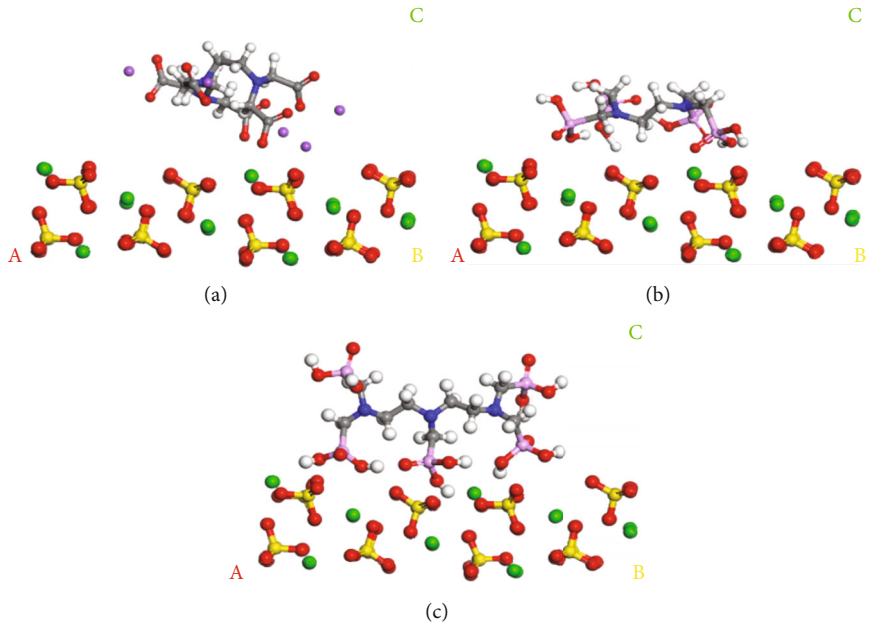

Figure 7: (101) Surface of barium sulfate is interacting with (a_3) DPTA-5Na, (b_3) EDTMPS, and (c_3) DTPMP.

Table 4: Adsorption energy (KJ/mol) of models of inhibitor-$BaSO_4$ surfaces.

(hkl)	DTPA-5Na	EDTMPS	DTPMP
(210)	−135.01	−132.12	−132.12
(001)	−209.27	−8.68	−4.82
(101)	−177.45	−52.10	76.19

in the absence and presence of inhibitors. In the blank case with no addition of inhibitors (Figure 3(a)), many dispersed needle-like and flake structures of crystals are observed. When 80 mg/L DTPMP is applied, the crystal morphology of $BaSO_4$ is obviously affected (Figure 3(b)). The existence of DTPMP in the system affects the lengthwise direction of crystals, and some flocculent and layered structures appear on the surface of $BaSO_4$ crystals. Significant changes in $BaSO_4$ crystals morphology are also obtained with the use of EDTMPS, which is shown in Figure 3(c). The $BaSO_4$ crystals have some star-shaped and laminar appearances. The changes of morphology of $BaSO_4$ crystal are probably due to the adsorption of DTPMP and EDTMPS by Ba^{2+} onto the interface or in the lattice of the crystal [26]. The adsorption behavior alters the crystal lattice and crystal growth of $BaSO_4$, which is also called lattice distortion [27, 28]. For comparison, as displayed in Figure 3(d), $BaSO_4$ crystals exhibit a topography, with many spherical distributed structures, which presumably indicate the anionic group of DTPA-5Na has reacted with $BaSO_4$ to form soluble and stable chelate. This phenomenon is usually regarded as solubilization [29, 30]. All results confirm that DTPA-5Na, EDTMPS, and DTPMP significantly influence the growth of $BaSO_4$.

3.4. Molecular Simulation. To further reveal the adsorption behavior of scale inhibitors on the ditch, a theoretical calculation is performed. The optimized configuration of DTPA-5Na, EDTMPS, DTPMP, and $BaSO_4$ are shown in Figure 4.For the three inhibitors to be adsorbed on $BaSO_4$ surface, they are placed horizontally on it, thus allowing them to relax initially. After optimization, the most stable configurations (with the lowest energy) of the $BaSO_4$ surface interacting with the inhibitors are displayed in Figures 5–7. It can be seen that none of them is severely distorted.

The adsorption energy of inhibitor-scale surface system is shown in Table 4. The negative E_{ads} values indicate that the adsorption process of the three inhibitors onto (210), (001), and (101) surfaces of $BaSO_4$ are spontaneous except for DTPMP onto the (101) surface of $BaSO_4$. The calculated adsorption energy of the inhibitors interacting with the three surfaces of $BaSO_4$ is in an order of DTPA-5Na < EDTMPS < DTPMP, which means DTPA-5Na is most likely to be absorbed by barium sulfate. In addition, DTPA-5Na is more liable to be absorbed onto the (001) surface of barium sulfate while DTPMP and EDTMPS are much easier to be adsorbed onto the (210) surface. Generally, interaction between scale surfaces and inhibitors is classified into physical adsorption and chemisorption. Physical adsorption occurs when the values of E_{ads} are higher than -40 kJ/mol. Chemisorption or a coordinate type of bond takes place when the values of E_{ads} is more negative than -40 kJ/mol [31, 32]. In our case, the DTPA-5Na is adsorbed to form new chemical bonds on the three surfaces of barium sulfate while DTPMP and EDTMPS are chemically adsorbed onto the (210) surface of barium sulfate. By contrast, DTPMP and EDTMPS are physically adsorbed onto the (001) surface of barium sulfate.

Moreover, the electron density difference and state density were calculated to locate the adsorption sites. As is shown in Figure 8(a), electron cloud of the sodium atom in DTPA-5Na is partially overlapped with that of the oxygen

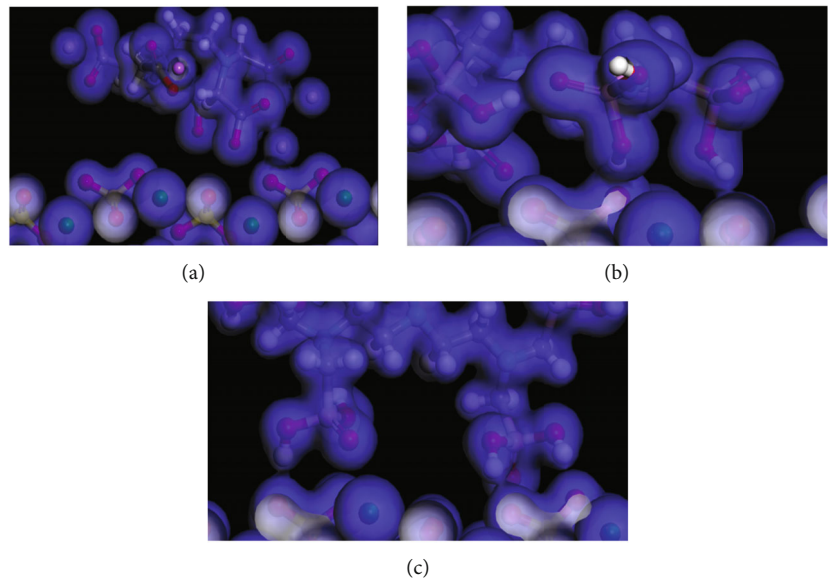

(a) (b) (c)

Figure 8: Difference charge density of (a) DTPA-5Na, (b) EDTMPS, and (c) DTPMP are absorbing on (001) surface of barium sulfate.

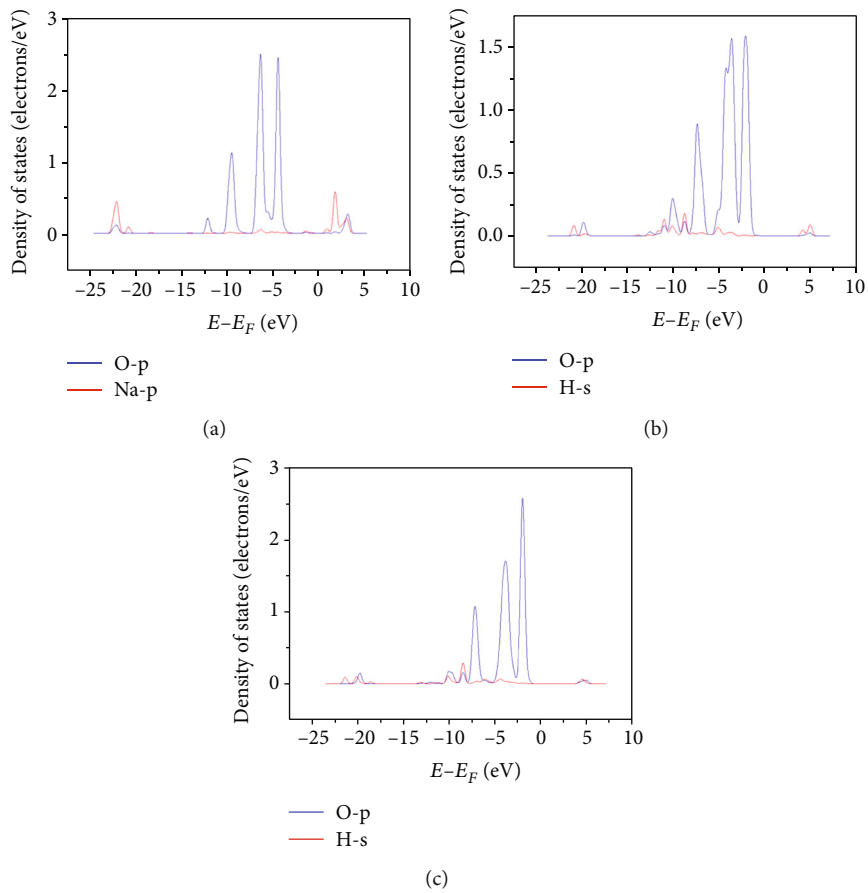

Figure 9: Density of states of sodium of (a) DTPA-5Na, hydrogen of (b) EDTMPS and (c) DTPMP is compared with oxygen atom of $BaSO_4$.

atom in $BaSO_4$, which illustrates that DTPA-5Na might interact with $BaSO_4$ by combining Na atoms with oxygen atoms. This result is further confirmed by DOS analysis. The p orbital of the sodium atom of DTPA-5Na is obviously overlapped with that of the oxygen of $BaSO_4$ from -24 eV to -4 eV, as is shown in Figure 9(a). By contrast, Figures 8(b)

and 8(c) show that the hydrogen atoms of phosphate groups of EDTMPS and DTPMP interact with oxygen atoms of $BaSO_4$. In addition, the interaction of hydrogen atoms and oxygen atoms was also confirmed by DOS analysis in Figures 9(b) and 9(c), which shows the s orbital of hydrogen atom of EDTMPS and DTPMP is obviously overlapped with p orbital of oxygen of $BaSO_4$ from -22 eV to 5.4 eV and -24 eV to 7 eV, respectively.

4. Conclusions

The major conclusions drawn from this study are summarized as follows.

(1) Barium sulfate is the main scaling type of the oilfield and the amount of scaling reaches its peak when injection water mixes with formation water at the ratio of 3 : 7

(2) Static tests show that the concentration of inhibitors obviously affects their antiscaling performance and the antiscaling ability of the three inhibitors experimentally is arranged by the order of DTPA-5Na > DTPMP > EDTMPS

(3) SEM micrographs suggest that EDTMPS, DTPMP, and DTPA-5Na visibly influence the process of crystal growth of $BaSO_4$ by lattice distortion and chelate effect

(4) Computational research indicates that DTPA-5Na is more likely to be chemisorbed onto the three surfaces of $BaSO_4$ while DTPMP and EDTMPS are chemically and physically absorbed onto the (210) and the (001) surface of $BaSO_4$, respectively. Difference charges calculation manifests that DTPA-5Na interacts with $BaSO_4$ by combining atoms of oxygen and sodium to form chemical new bonds, while EDTMPS and DTPMP interact with $BaSO_4$ by combining hydrogen atoms of phosphate groups and atoms of oxygen. All results are confirmed by DOS analysis

Data Availability

The data are not available due to commercial restrictions.

Conflicts of Interest

The authors declare that they have no known competing financial interests or personal relationships that could have appeared to influence the work reported in this paper.

Authors' Contributions

Haitao Li is responsible for the gathering of resources, the supervision, and the software analysis. Ran Li is responsible for the writing of the original draft, the investigation, and the formal analysis.

Acknowledgments

We also thank Southwest Petroleum University for providing study assistance.

References

[1] M. M. Vazirian, T. V. J. Charpentier, M. de Oliveira Penna, and A. Neville, "Surface inorganic scale formation in oil and gas industry: as adhesion and deposition processes," *Journal of Petroleum Science and Engineering*, vol. 137, pp. 22–32, 2016.

[2] B. S. Bageri, A. R. Adebayo, A. Barri et al., "Evaluation of secondary formation damage caused by the interaction of chelated barite with formation rocks during filter cake removal," *Journal of Petroleum Science and Engineering*, vol. 183, p. 106395, 2019.

[3] W. Kang, T. Wang, H. Zhang et al., "A dynamic scale location monitor method to predict oilfield blockage during water flooding," *Journal of Petroleum Science and Engineering*, vol. 191, p. 107168, 2020.

[4] D. Coll de Pasquali, E. Horai, M. I. Real et al., "Chemical dissolution of oilfield strontium sulfate ($SrSO_4$) scale by chelating agents," *Applied Geochemistry*, vol. 106, pp. 134–141, 2019.

[5] L. Mahmoodi, M. R. Malayeri, and F. F. Tabrizi, "Abatement of scale precipitation in oilfields using green scale inhibitors," *Journal of Petroleum Science and Engineering*, vol. 208, p. 109237, 2022.

[6] A. B. BinMerdhah, "Inhibition of barium sulfate scale at high-barium formation water," *Journal of Petroleum Science and Engineering*, vol. 90-91, pp. 124–130, 2012.

[7] T. Chen, A. Neville, and M. J. Yuan, "Engineering, calcium carbonate scale formation—assessing the initial stages of precipitation and deposition," *Journal of Petroleum Science and Engineering*, vol. 3, no. 46, pp. 185–194, 2005.

[8] T. Guo, H. Gu, and N. Wang, "Dissolution behavior of DTPA-promoted barium slag and synthesis of submicron $BaSO_4$ particles," *Journal of Cleaner Production*, vol. 362, p. 132482, 2022.

[9] A. Khormali, G. Bahlakeh, I. Struchkov, and Y. Kazemzadeh, "Increasing inhibition performance of simultaneous precipitation of calcium and strontium sulfate scales using a new inhibitor – laboratory and field application," *Journal of Petroleum Science and Engineering*, vol. 202, p. 108589, 2021.

[10] D. Darling and R. Rakshpal, *Green Chemistry Applied to Corrosion and Scale Inhibitors*, One Petro, 1998, CORROSION 98,.

[11] U. Z. Husna, K. A. Elraies, J. A. Shuhili, and A. A. Elryes, "A review: the utilization potency of biopolymer as an eco-friendly scale inhibitors," *Journal of Petroleum Exploration and Production Technology*, vol. 12, no. 4, pp. 1075–1094, 2022.

[12] D. Zeng and H. Yan, "Study on an eco-friendly corrosion and scale inhibitor in simulated cooling water," *American Journal of Engineering Research*, vol. 2, no. 5, pp. 39–43, 2013.

[13] D. Liu, W. Dong, F. Li, F. Hui, and J. Lédion, "Comparative performance of polyepoxysuccinic acid and polyaspartic acid on scaling inhibition by static and rapid controlled precipitation methods," *Desalination*, vol. 304, pp. 1–10, 2012.

[14] B. Zhang, L. Zhang, F. Li, W. Hu, and P. M. Hannam, "Testing the formation of Ca–phosphonate precipitates and evaluating the anionic polymers as Ca–phosphonate precipitates and

CaCO3 scale inhibitor in simulated cooling water," *Corrosion Science*, vol. 52, no. 12, pp. 3883–3890, 2010.

[15] Y. Zuo, W. Yang, K. Zhang, Y. Chen, X. Yin, and Y. Liu, "Experimental and theoretical studies of carboxylic polymers with low molecular weight as inhibitors for calcium carbonate scale," *Crystals*, vol. 10, no. 5, p. 406, 2020.

[16] R. Cisneros-Dévora, R. Hernández-Altamirano, J.-M. Martínez-Magadán et al., "Development through computational design of a new terpolymer with anti-scale properties applied to the oil production assurance process," *Fuel*, vol. 282, p. 118832, 2020.

[17] R. Jalab, M. A. Saad, I. A. Hussein, and A. T. Onawole, "Calcite scale inhibition using environmental-friendly amino acid inhibitors: DFT investigation," *ACS Omega*, vol. 6, no. 47, pp. 32120–32132, 2021.

[18] F. Gaining, C. Yu'e, and Z. Lihua, "An improvement in complexometric titration for evaluating the efficiency of scale inhibitors., Oilfiled," *Chemistry*, vol. 21, no. 3, pp. 284–286, 2004.

[19] B. Delley, "An all-electron numerical method for solving the local density functional for polyatomic molecules," *The Journal of Chemical Physics*, vol. 92, no. 1, pp. 508–517, 1990.

[20] B. Delley, "From molecules to solids with the DMol 3 approach," *The Journal of Chemical Physics*, vol. 113, no. 18, pp. 7756–7764, 2000.

[21] J. P. Perdew, K. Burke, and M. J. Ernzerhof, "Generalized gradient approximation made simple," *Physical Review Letters*, vol. 77, no. 18, pp. 3865–3868, 1996.

[22] N. L. Allan, A. L. Rohl, D. H. Gay, C. R. A. Catlow, R. J. Davey, and W. C. Mackrodt, "Calculated bulk and surface properties of sulfates," *Faraday Discussions*, vol. 95, pp. 273–280, 1993.

[23] H. Li, X. Meng, and R. Li, "Experimental study on factors affecting the effect of barium sulfate scale inhibition," *Journal of Southwest Petroleum University*, vol. 36, no. 1, pp. 139–144, 2014.

[24] F. Jones, W. R. Richmond, and A. L. Rohl, "Molecular modeling of phosphonate molecules onto barium sulfate terraced surfaces," *The Journal of Physical Chemistry B*, vol. 110, no. 14, pp. 7414–7424, 2006.

[25] V. Celli and N. Flytzanis, "Motion of a screw dislocation in a crystal," *Journal of Applied Physics*, vol. 41, no. 11, pp. 4443–4447, 1970.

[26] Y. Liu, A. T. Kan, M. B. Tomson, and P. Zhang, "Interactions of common scale inhibitors and formation mineral (calcium carbonate): sorption and transportability investigations under equilibrium and dynamic conditions," *Journal of Petroleum Science and Engineering*, vol. 215, p. 110696, 2022.

[27] D. Hasson, D. Bramson, B. Limoni-Relis, and R. Semiat, "Influence of the flow system on the inhibitory action of $CaCO_3$ scale prevention additives," *Desalination*, vol. 108, no. 1-3, pp. 67–79, 1997.

[28] K. Popov, M. Oshchepkov, E. Afanas'eva, E. Koltinova, Y. Dikareva, and H. Rönkkömäki, "A new insight into the mechanism of the scale inhibition: DLS study of gypsum nucleation in presence of phosphonates using nanosilver dispersion as an internal light scattering intensity reference," *Colloids and Surfaces A: Physicochemical and Engineering Aspects*, vol. 560, pp. 122–129, 2019.

[29] G. Jing, S. Tang, and X. Li, "Analysis and inhibition of scale accumulation for a producing well in the Daqing Oilfield," *Petroleum Science and Technology*, vol. 31, no. 17, pp. 1772–1777, 2013.

[30] J. Yang, Y. Chen, X. Zhao, C. Ma, Y. Li, and X. He, "Controlled-release chemicals in oilfield application: a review," *Journal of Petroleum Science and Engineering*, vol. 215, p. 110616, 2022.

[31] F. M. Donahue and K. Nobe, "Theory of organic corrosion inhibitors," *Electrochemistry*, vol. 112, no. 9, p. 886, 1965.

[32] E. Khamis, F. Bellucci, R. Latanision, and E. S. H. El-Ashry, "Acid corrosion inhibition of nickel by 2-(triphenosphoranylidene) succinic anhydride," *Corrosion*, vol. 47, no. 9, pp. 677–686, 1991.